COMPLESSITÀ NEI SISTEMI SOCIALI

LORENZO DALL'AMICO
ISI Foundation

Note per il corso in Fisica dei sistemi complessi

Università di Torino
April 8, 2024

Lorenzo Dall'Amico: *Complessità nei sistemi sociali*

CONTENTS

ACRONYMS

F2F *Face-to-face*

ER *Erdős-Rényi*

NMF *naïve mean field*

BP *belief propagation*

SIR *Susceptible-Infected-Recovered model*

GW *Galton Watson tree*

GFT *Graph Fourier transform*

CD *Community detection*

AMI *Adjusted mutual information*

DCSBM *Degree corrected stochastic block model*

SC *Spectral clustering*

SYMBOLS

- $\delta_{a,b}$ is the Kroeneker delta equal to 1 if $a = b$ and equal to 0 otherwise.
- $\Lambda(M)$ is the set of eigenvalues of a matrix M. $\lambda_i(M)$ is the i-th (smallest or largest, according to the context) eigenvalue of M
- The spectral radius of M (largest eigenvalue) is denoted with $\rho(M)$.
- With the notation $\mathbf{1}_n$ we denote the all-ones vector of size n.
- The entry-wise Hadamard product is denoted with $\circ$.
- The set of the first n integers is denoted with $[n]$.
- We adopt the Landau notation for the asymptotic behavior of variables. In particular $x = O_n(y)$ is equivalent to $\lim_{n\to\infty} \frac{x}{y} = c$ for some finite c. The notation $x = o_n(y)$ instead means $\lim_{n\to\infty} \frac{x}{y} = 0$.
- The set of neighbors of a node i on a graph is $\partial i = \{j \in \mathcal{V} \,:\, A_{ij} = 1\}$

1 TEMPORAL GRAPHS

1.1 WHY TEMPORAL GRAPHS?

Graphs are an essential mathematical tool to represent interacting systems. When using static graphs, the interactions between two nodes is often represented as a single Boolean variable determining whether or not those two nodes interacted with one another. Yet, we can think of many examples in which this variable should depend on time. Think of a graph in which an interaction between two people is a phone call. In most instants, for most people, no interactions are recorded at all, and, in all cases at most one interaction per time may occur. So, how would we determine the Boolean interaction variable? One approach would be to aggregate time as determine that two people interacted if they had enough phone calls during a specific time window. In this way, connections are created between people that frequently call each other, but we loose an important piece of information: the order of events. Imagine an event like the fire of Notre Dame de Paris: in few moments people witnessing the fire spread the news to their contacts who, themselves reported to others in chain. If we had no idea of what happened and what is the content of the calls or messages, we could actually retrieve the geographical location from which the burst of information was initiated by retracing backwards the chain of events. If instead we use a static representation of the graph as we did earlier, all this information would be lost. A temporal graph is then an object capable of representing the interactions between the elements of a system together with a time stamp. Besides communication graphs, other notable examples are face-to-face proximity graphs, biological graphs, ecological graphs and many others.

A pictorial representation of a chain of calls

As we will show in the remainder, in some cases it is necessary to keep the temporal dimension into account if one wants to understand the process happening on top of a graph. This is due to the fact that links may have

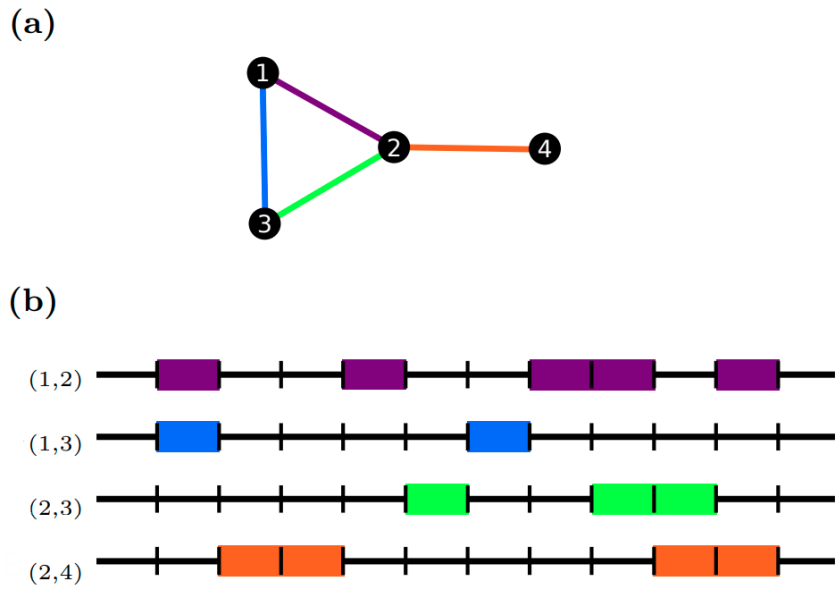

Figure 1.1: **A pictorial representation of a temporal graph**. (a) A graph with 4 nodes with $\mathcal{V} = \{1,2,3,4\}$ and $\mathcal{E} = \{(1,2),(1,3),(2,3),(2,4)\}$. (b) the temporal activation patterns of each edge (with color code). The x axis represents time. Picture taken from *Gauvin et al., Randomized reference models for temporal graphs.*

a causal relation (like the phone calls in the Notre Dame example) or simply because the aggregated static graph may be non representative of the interactions at any time stamp. We will then discuss how to mathematically define and represent temporal graphs, a relevant example of how to measure them and show some peculiar properties of temporal graphs.

1.2 REPRESENTING TEMPORAL GRAPHS

Let us consider a set of nodes $\mathcal{V}$ and a set of edges $\mathcal{E}$ connecting the nodes. Given a suited definition of interaction for our problem and a time window, $\mathcal{E}$ is the set of all pairs of nodes (i,j) that interacted at least once in the considered time window. We now want to add the notion of *when* these interactions occurred. Each edge (i,j) can appear multiple times and for each interaction we can consider a time t at which the interaction begun and a time duration τ.[1] We can then represent a temporal graph as a sequence of *temporal edges* in the form (i,j,t,τ). Figure 1.1 gives a pictorial representation of the temporal edges of a graph with 6 nodes. We now provide a more formal definition of a temporal graph.

1 We could equivalently replace τ with the time t_e at which the interaction ended.

Temporal graphs

A temporal graph is a tuple $\mathcal{G}(\mathcal{V}, \mathcal{E}_t)$, where $\mathcal{V}$ denotes the set of n nodes and $\mathcal{E}_t$ of temporal edges. Each $e \in \mathcal{E}_t$ can be written as (i, j, t, τ) where $i, j \in \mathcal{V}$, t is a time-stamp and $\tau \in \mathbb{R}^+$ is a positive interaction duration, implying that the link between i and j was active from t to $t + \tau$. If a node has at least one connection at time t we say it is *active* at time t and it is inactive otherwise.

Temporal graphs

One can generalize the concept of adjacency matrix to the temporal setting by letting

$$\tilde{A}_{ij}^{(t)} = \begin{cases} 1 & \text{if } \exists\, e = (i, j, t_0, \tau) \in \mathcal{E}_t \text{ s.t. } t \in [t_0, t_0 + \tau] \\ 0 & \text{else.} \end{cases}$$

Temporal adjacency matrix

In this representation, however, time is kept as a continuous variable and, even for a finite observation time, we obtain an infinite number of adjacency matrices. For this reason, the snapshot representation – that uses a discrete notion of time – may be more suited. In particular, we assume that the interaction duration τ is a multiple of a unit Δt that sets the temporal resolution of the graph. Let us define the concept of snapshot graphs, pictorially visualized in Figure 1.2.

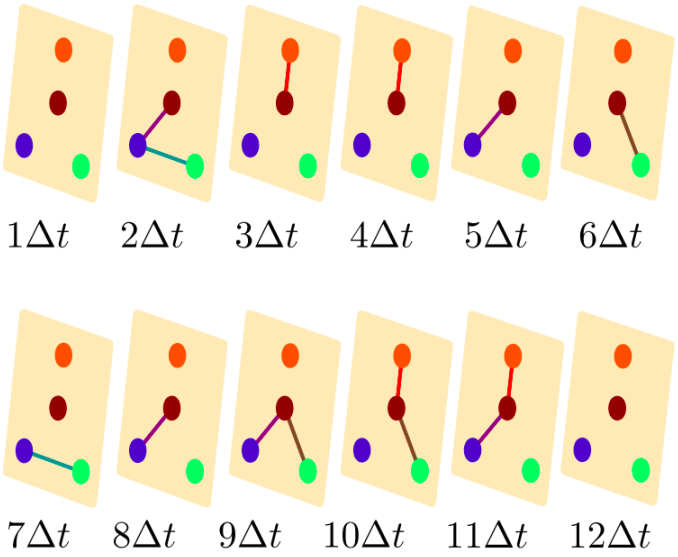

Figure 1.2: **A pictorial representation of a snapshot graph**. This plot represents the same graph of Figure 1.1 in which time was already discretized for convenience. Each *slice* corresponds to a different time step in which the edges progressively are activated. Picture taken from *Gauvin et al., Randomized reference models for temporal graphs.*

Snapshot graphs

Snapshot graphs

A snapshot graph is a tuple $\mathcal{G}(\mathcal{V}, \mathcal{E}_t)$, where $\mathcal{V}$ denotes the set of n nodes and $\mathcal{E}_t$ of temporal edges. Each $e \in \mathcal{E}_t$ can be written as (i, j, t) where $i, j \in \mathcal{V}$, t is a *discrete* time-stamp and models an instantaneous interaction between i, j at time t.

With this representation at hand, one can obtain the adjacency matrix representation of a temporal graph as follows

The snapshot adjacency matrix

$$A_{ij}^{(t)} = \begin{cases} 1 & \text{if } (i, j, t) \in \mathcal{E}_t \\ 0 & \text{else.} \end{cases}$$

In this way we obtain a sequence of T adjacency matrices $\{A^{(t)}\}_{t \in 1,\dots,T}$, where T is the total number of snapshots. A natural question that poses is how which of the two representations is more appropriate and how much information is lost when choosing to discretize time. We address this point in the following remark.

Discretizing time

Discretizing time

If we want to choose a discrete representation of time, the natural questions that arise are how to choose Δt, the minimal interaction duration and how much do we loose in performing this simplification. The first point we want to raise is that any measured quantity (including time) is not truly continuous and it is bounded by a resolution that makes time discrete by design. So, in all cases, one can say Δt is the measurement instrument resolution and the snapshot representation is always appropriate. Yet, if Δt is much smaller than the total observation time, the number of time frames T – even if finite – will tend to be very large, hence untractable. So, setting a longer Δt might be more appropriate in some cases and the choice of a good Δt is necessarily problem-dependent because Δt determines the scale at which we consider interactions to be *simultaneous*.

The coupling between the process and graph dynamics

Let us make two examples to make this point clearer. Suppose we have two spreading phenomena: in one case the propagation of a piece of information (such as the fire of Notre Dame) and in the other a flu-like illness transmission. In the former case, the propagation of the information from one person to the other moves very fast and so Δt must be small, in the order of seconds/minutes to capture the rapid dynamics of the news propagation. If we consider the flu-like propagation, instead, we know that a person, after being infected, is not typically able to infect someone for a couple of days, hence we can set Δt of the order of one day, assuming that one cannot change its own infectious state in the course of a day. So, summarizing, the proper time aggregation depends on the time-scale of the dynamic

process happening on top of the graph. If this process if much slower than the temporal evolution then we can simply aggregate the graph. If instead the two time scales (of the process and of the graph evolution) are similar, then we have an interesting coupling that must be taken into account.

To conclude this remark, there is still a quantity we want to preserve when we aggregate time, that is the cumulative interaction duration: what do we do with all interactions so that $\tau < \Delta t$? Also in this case the answer depends on the problem under consideration. Take for instance the flu propagation with a time aggregation of 24 hours. If an infectious individual has a interaction with a susceptible one, the interaction duration is key to determine the probability of infection: an hour-long interaction is much more likely to propagate the disease than a minute-long interaction and all interactions will be shorter than Δt in this case. To preserve this piece of information, we might want to associate a weight to each edge, representing the cumulative interaction duration. We relate the continuous time and snapshot adjacency matrices as follows

The weighted aggregated graph

$$W_{ij}^{(t)} = \int_{t}^{t+\tau_0} dt' \, \tilde{A}_{ij}^{(t')}.$$

If this representation may seem very reasonable, it must be noted that is not the only admissible one: in the case of the propagation of sexual diseases, for instance, the interaction duration is not relevant and may simply want to keep a Boolean representation of the edges, without attributing any weight.

Now that we have introduced some of the main concepts related to temporal graphs, let us consider the specific set of proximity graphs as a case study, first describing a method to measure these graphs and then using the open source, real data to describe some relevant properties.

1.3 MEASURING PROXIMITY GRAPHS

In proximity graphs the edges represent a *Face-to-face* (F2F) contact between two persons. The interest of this type of graphs resides in the fact that F2F interactions are the vehicle of human communication and of infectious diseases and, more generally, they quantify how humans interact with one another. Measuring *Face-to-face* (F2F) proximity graphs is, however, a very challenging task. Among the most used approaches to quantify them we have the use of questionnaires in which the interactions one has are self-reported. It was shown that this method is biased towards long interactions – in the sense that short interactions tend to be forgotten – and can achieve a low temporal resolution. A very important contribution to the field of measur-

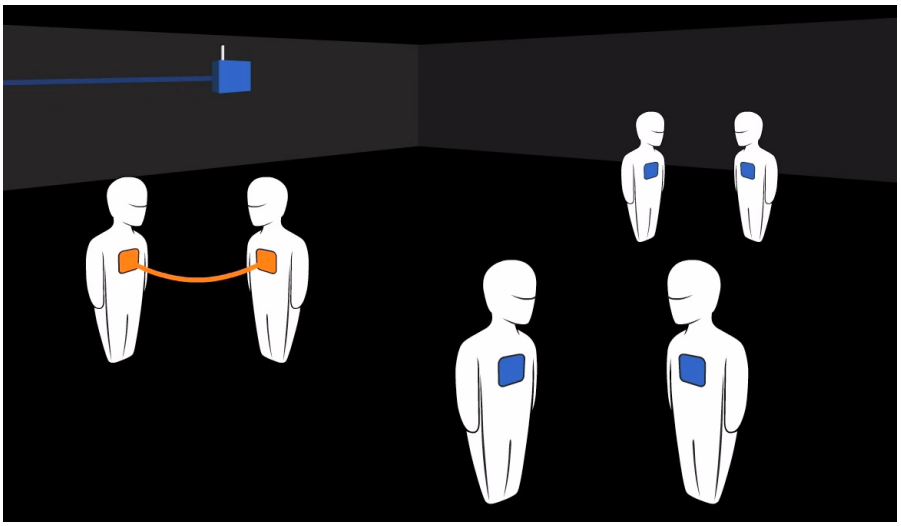

Figure 1.3: **Pictorial example of the use of SocioPatterns proximity sensors**. Six people in a room wearing a proximity sensor. The orange ones (with the line), indicate a recorded F2F interactions between two individuals. Picture taken from http://www.sociopatterns.org/.

ing F2F proximity graphs was made with the creation of the SocioPatterns collaboration by the ISI Foundation.

The SocioPatterns collaboration

SocioPatterns was formed in 2008 and developed wearable proximity sensors that are capable to *measure* temporal proximity graphs. Their functioning is based on the transmission and exchange of information packets using radio-frequency electromagnetic waves. Briefly speaking, each device is associated with a code and continuously switches from a *listener* to a *speaker* mode. When it is in the *speaker* mode it emits an information packet containing its own code and the power at which the signal was emitted. When it is in listener mode, instead, the device intercepts the packets emitted by the "speakers" and records on its memory the code and the power declared, the time stamp at which this interaction occurs as well as the power of the received signal. The devices have to be worn on the chest of the participants and, by design, record F2F proximity. Figure 1.3 shows a demo of the functioning of the SocioPatterns proximity sensors.

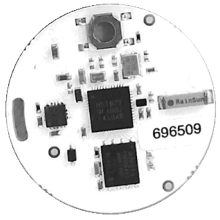

A proximity sensor

Inside the memory of each sensor we then have a list of entries of the type $(j, \mathrm{pow}_{\mathrm{tr}}, \mathrm{pow}_{\mathrm{rec}}, t)$, where j is the code of the sensor that emitted the signal, $\mathrm{pow}_{\mathrm{tr}}$ is the transmission power, $\mathrm{pow}_{\mathrm{rec}}$ is the received power and t is the time-stamp that has a temporal resolution of 20 seconds. Looking at the difference $\mathrm{pow}_{\mathrm{tr}} - \mathrm{pow}_{\mathrm{rec}}$ one can measure the attenuation of the signal and filter out the interactions that are too attenuated, thus keeping only those that happened at a distance within approximately 2 meters. From this we can create a snapshot graph with $\Delta t = 20\ s$ as described above.

The SocioPatterns sensors have been used in several contexts, including schools, hospitals, offices and rural African villages among others. They constitute a well known benchmark of temporal graph measurement that has

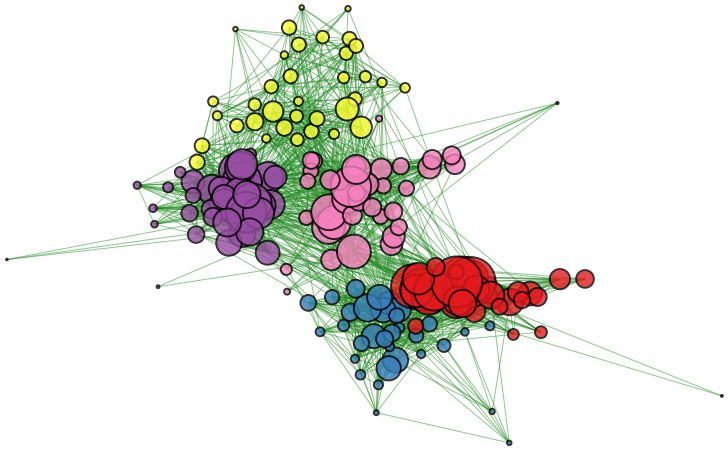

Figure 1.4: **The *School* dataset**. Pictorial representation of the *School* dataset (see Table 1.1) aggregated over all the observation time. The size of each node is the determined by the total interaction time of that node, while the color is determined by the class the student belongs to.

been used in many applications and many of the collected datasets are publicly available at http://www.sociopatterns.org/datasets/. We will make use of some of these data to study some relevant properties of temporal graphs. Table 1.1 summarizes some descriptive properties of the considered graphs, while Figure 1.4 shows the aggregated graph collected in a high school.

Name	n	Observation time	Description
School	180	from a Monday to the Tuesday of the following week in November 2012.	interactions between students in a high school in Marseilles, France belonging to 5 classes.
Office	92	June 24 to July 3, 2013	interactions between individuals measured in an office building in France
Village	86	between 16th December 2019 and 10th January 2020	interactions between the people of Mdoliro village in Dowa district in the Central Region of Malawi.
Conference	405	June 4-5, 2009	interactions at the SFHH conference in Nice

Table 1.1: **Summary statistics of the *SocioPatterns* temporal networks**. The first column indicates the name used in these notes. The column indexed by n indicates the number of nodes appearing in the graph. The column *Observation time* describes the experiment duration, while *Description* provides a few details on the context of the data collection. For more information, refer to the SocioPatterns website.

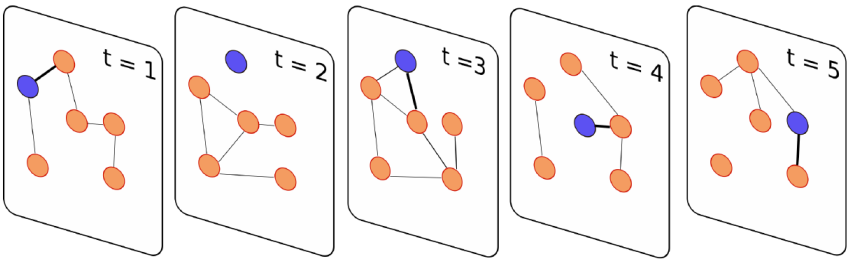

Figure 1.5: **Time respecting paths**. Five snapshots of a temporal graph in which unoccupied nodes are depicted in orange at each time, while the currently occupied node is in blue. A larger width is used to highlight the edge that causes the transition.

1.4 PROPERTIES OF TEMPORAL GRAPHS

We now proceed to describe some important concepts that characterize temporal graphs and use the four aforementioned datasets to show them on empirical data.

TIME-RESPECTING PATHS

When we consider a graph $\mathcal{G}(\mathcal{V}, \mathcal{E})$, we define a path on it as an ordered sequence of nodes $\{i_1, i_2, \dots, i_T\}$ for that, for all $p \in [T]$, $i_p \in \mathcal{V}$ and for all $p \in [T-1]$, $(i_p, i_{p+1}) \in \mathcal{E}$. In words, every step of a path allows one to only move from a node to one of its neighbors. When we consider a temporal graph, instead, we must generalize the concept of path, to encode the role played by time, introducing the *time-respecting paths*.

Time respecting paths

Time respecting paths

Given a temporal graph $\mathcal{G}(\mathcal{V}, \mathcal{E}_t)$, we denote a time respecting path as $\{i_1(t_1), i_2(t_2), \dots, i_T(t_T)\}$ if it satisfies the following conditions

- For all $p \in [T]$, $i_p \in \mathcal{V}$: the path is defined on the graph nodes.
- For all $p \in [T-1]$, $t_p < t_{p+1}$: these two times indicate the beginning of the residency on the respective nodes and time must be increasing.
- For all $p \in [T-1]$, $\exists\, t_0, \tau$ s.t. $(i_p, i_{p+1}, t_0, \tau) \in \mathcal{E}_t$ and $t_{p+1} \in [t_0, t_0 + \tau]$: the transition between one node and the other can only take place at a time at which the two nodes are connected.

This definition is given for a continuous time representation but it can simply be adapted to the discrete one. For this case, we give a simple representation of a time respecting path in Figure 1.5.

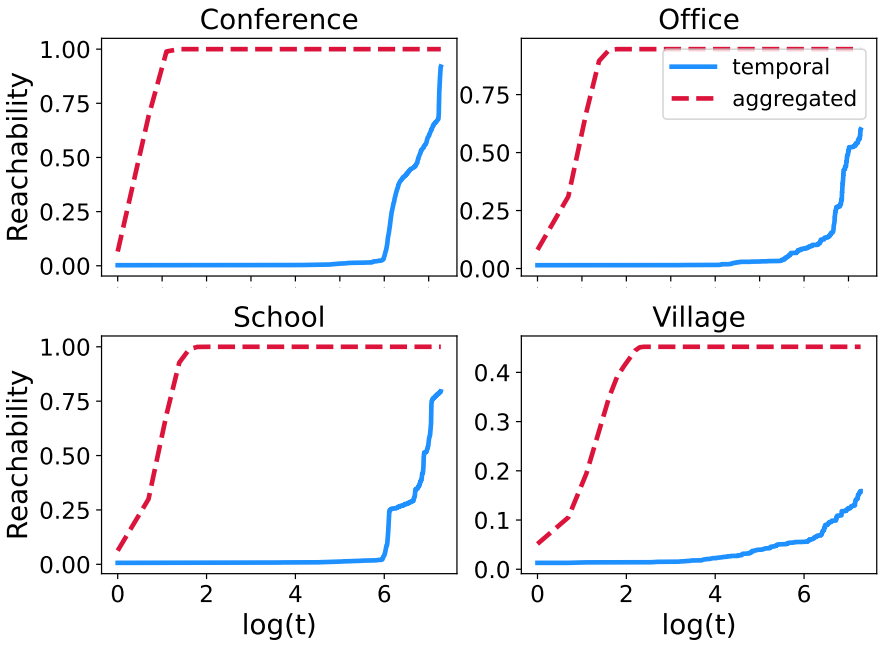

Figure 1.6: **Time-respecting vs aggregate reachability**. Each plot refers to one of the 4 *SocioPatterns* datasets described in Table 1.1, considering the first 8 hours of measurements. The red dashed line is the average of the reachability matrix R_t defined in Equation (1.1) as function of time, using for all t A_t the weighted aggregated matrix over all the observation period. The blue continuous line, instead, is obtained from the snapshot adjacency matrices and encodes time-respecting paths.

Given a sequence of adjacency matrices, we now define the *reachability matrix* R_t as follows

$$R_t = \text{sign}\left[\prod_{t'=1}^{t}(A_{t'} + I_n)\right], \tag{1.1}$$

Reachability matrix

where I_n is the identity matrix, the sign function has to be considered entry-wise, while the product has to be taken from right to left, *i.e.* $\prod_{t=1}^{3} A_t = A_3 A_2 A_1$. The entry $R_{t,ij}$ equals 1 if there exists a time-respecting path of length smaller or equal to t that allows one to go from i to j.

Time-respecting paths are not symmetric

An important fact related to this matrix is that it is not necessarily symmetric. This comes from the fact that the product of matrices (such as the A_t's) is symmetric only if the matrices commute. This is not the case in general and it implies that if there is a time-respecting path from i to j, that does not imply that there exists also a time-respecting path from j to i.

By taking the average of the reachability matrix, we also have a measure of how well its nodes are connected. Figure 1.6 compares the reachability on the 4 real temporal graphs described above with the one obtained on their aggregated version and clearly shows that temporal graphs have a lower reachability. This is because the valid time-respecting paths are constrained

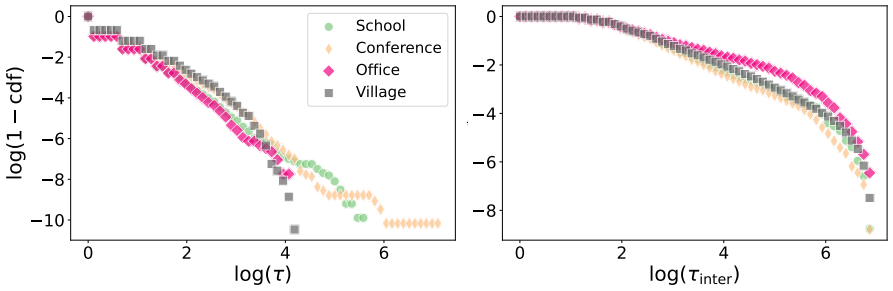

Figure 1.7: **Event and inter-event duration distributions**. The figures show the scatter plot in log-log scale of the interaction duration (left) and inter-event duration (right) distributions vs the $1 - cdf$, *i.e.* the complementary of the cumulative density function. Each line refers to one of the datasets described in Table 1.1 and is color and marker coded.

and are only a subset of all the possible paths that one can perform on the aggregate version of the graph. This is an important ingredient to consider when coupling a dynamic process with the graph, because only a fraction of all possible paths can actually take place.

DURATION DISTRIBUTION AND BURSTINESS

We now focus on a very peculiar aspect of contact graphs, that is the contact duration distribution. It has been observed in many instances (with no apparent exception) that this distribution is very broad and follows approximately a power law decay that appears to be a universal behavior. Figure 1.7 (left plot) shows in log-log scale 1 minus the cumulative density function vs the interaction duration and confirms this trend, since the relation is approximately linear in the logarithmic scale. This is an important observation, because it tells us that very long interactions are much more common than what we would expect for a thin tail distribution, such as the Poisson. The consequence is that, if we have a process that needs a minimal time of interaction to consider the interaction to be valid, then, in practice, even if the threshold is very large, there will be valid interaction edges with high probability. On the other hand, we also know that most of the distribution is concentrated around small values.

$1 - \mathrm{cdf}(x) = \mathbb{P}(\tau \geq x)$

A similar behavior is observed for the inter-event duration distribution. We define the inter-event duration as the time elapsed between two successive interactions of the same pair of nodes (ij). Since this distribution is broad, we say that the interaction dynamics is *bursty*, *i.e.* that typically we have an alternation of time intervals in which the activity is very low and some in which it is very high. To best understand the effect that a bursty dynamics may have on a process, let us consider the following example.

Suppose we have a quantity $\mathscr{Q}$ that is increased by one unit every time there is a interaction and it is decreased by a factor α for each time step in which no interaction occurs. If $\mathscr{Q}$ exceeds a threshold value $\mathscr{Q}_{\mathrm{th}}$, then some

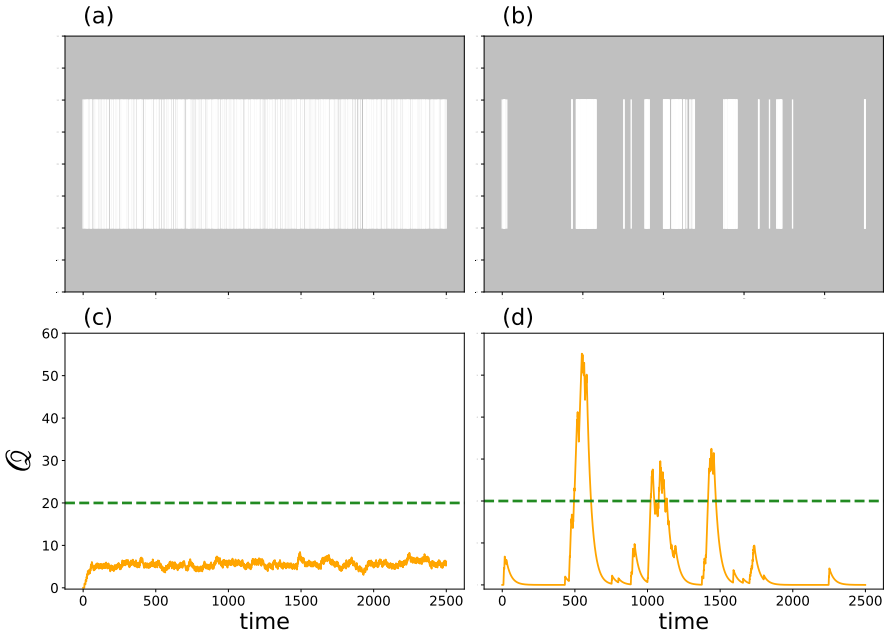

Figure 1.8: **The effect of bursty dynamics**. The first row represents a temporal time series for (a) a Poisson process and (b) the interaction times of a node of the *Conference* graph (see Table 1.1. Each horizontal line indicates an active time. The second line displays the dynamics of a quantity $\mathcal{Q}$ evolving according to the process described in the main text for (c) the Poisson dynamics of (a), and for (d) the bursty dynamics of (b). The horizontal dashed line indicates an arbitrary selected threshold value that triggers some process when $\mathcal{Q} > \mathcal{Q}_{\text{th}}$. Image adapted from *Holme, Saramaki, Temporal networks.*

process is triggered otherwise it is not. In Figure 1.8 we compare this dynamical process on a Poisson temporal series made of 362 interaction events with one extracted from an individual activity pattern of the *Conference* graph. The bottom plots clearly evidence that the bursty dynamics, being highly concentrated in some time regions, allows one to go beyond the threshold several times, while this does not happen to the Poisson distribution.

A method to measure the burstiness level of a time series is as follows

$$B = \frac{s - m}{s + m},$$

where s and m are the standard deviation and mean of the inter-event duration distribution, respectively. For a periodic process, $s = 0$ and $B = -1$, while for the burstiest of processes, $s \to \infty$ and $B \to 1$. In our case, the Poisson dynamics of Figure 1.8(a) has $B = -0.45$, while the one of Figure 1.8(b) has $B = 0.70$.

1.5 CONCLUSION

Temporal networks are a powerful tool to model complex dynamical systems. Empirical networks often show very broad distribution of the interaction duration as well as bursty dynamics. These features are of great importance to some dynamical processes that may unfold on networks and the temporal framework is a relevant generalization of static graphs. However, the dynamic component of graph evolution must always be compared with the typical time scale of the process unfolding over the graph in order to understand whether it is necessary to have an additional layer of complexity given by time or, more in general, to choose an appropriate time discretization to perform the analysis.

1.6 REFERENCES

- P. Holme, J. Saramäki, *Temporal networks*. Physics reports, 519(3), 97-125 2012.
  This is *the* reference for an introduction to temporal graphs.

2 EPIDEMICS ON NETWORKS

2.1 EPIDEMICS

Epidemiology is a branch of science that studies the determinants, distribution and dynamics of a propagation process in a population. Given its relation to a whole population, epidemiology is, by design complex and of great interest when shaping public health policies. We will focus on infectious disease epidemiology, *i.e.* on illnesses that can be transmitted from one person to the other. Notable examples include the bubonic plague, smallpox, the Spanish flu, HIV, influenza and, of course, Covid. Even though we will mainly have in mind "illness" propagation, a similar if not identical mathematical framework can be adopted to anythings that propagates through interactions, such as opinions, computer viruses or information.

Let us now describe in deeper detail some fundamental elements of epidemics and their modeling.

2.1.1 EPIDEMIC MODELING

The basic medical observation that we want to model and capture is that when a person is "sick" – for instance it is positive to influenza – and it is in contact with a person who is not – and never was – then it can pass the infection over to the healthy person. The meaning of "contact" depends on the disease we are considering: think to the extreme difference there

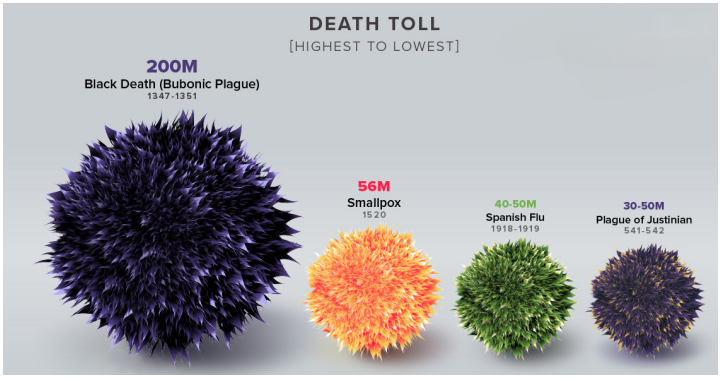

Figure 2.1: **The deadliest pandemics in history**.
Source: visualcapitalist.com/history-of-pandemics-deadliest

is between the HIV and the flu transmissions. Nonetheless, the dynamic processes we have in mind are very similar. We introduce the *Susceptible-Infected-Recovered model* (SIR), a cornerstone of epidemic modeling.

We define three possible states every individual can be in: S, susceptible; I, infected; R recovered. Susceptible people are healthy individuals that can contract the disease. Infectious ones are those who currently carry the disease and can spread it out when they interact with a susceptible individual. The recovered people, instead, are those who used to be infectious and now can no longer be infected. There are two important parameters that take part to this model: β that is the probability *per unit time* to infect a susceptible person and μ, the probability *per unit time* to recover. We can summarize the SIR model with the following equation

The SIR model

$$S + I \xrightarrow{\beta} 2I$$
$$I \xrightarrow{\mu} R$$

The parameters β, μ are disease-dependent and tell us how easily the infection runs across the population. Intuitively, if $\beta \gg \mu$ we are in a situation in which people get infected at a much faster pace than they recover. As a consequence, the epidemic will swiftly spread across the population. On the opposite, if $\mu \ll \beta$ people simply recover very quickly and the epidemic dies out. This concept, that we delineated in intuitive terms, is the so-called epidemic threshold that determines the necessary and sufficient condition for an epidemic spreading to occur and that we now more formally define.

2.1.2 THE EPIDEMIC THRESHOLD

We consider a population in which everybody is susceptible. This condition is a stationary state, because no infection can occur among susceptible people, or, in other words

$$S + S \longrightarrow 2S.$$

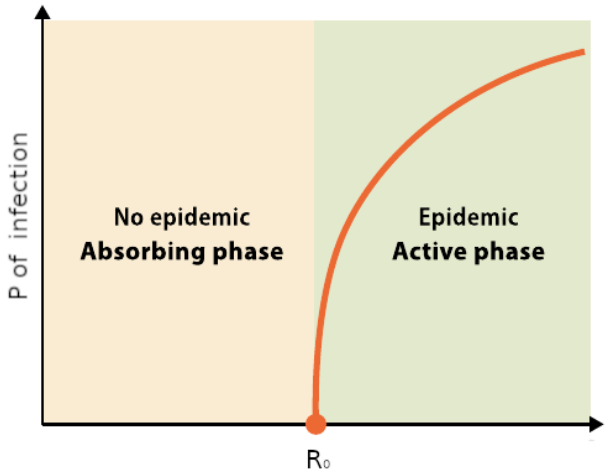

Figure 2.2: **Epidemic threshold phase diagram**. Below the critical value of R_0 we are in an absorbing phase in which there is no epidemic, while for R_0 larger than the critical value, the probability that each node has of being infected is non-null. Source: Satorras, Castellano, Van Mieghem, Vespignani. *Epidemic processes in complex networks.*

We now perturb this state introducing few infectious individuals and ask ourselves whether the system will fall back to an equilibrium having most people being unaffected by the disease, or, if it will spread hitting a large portion of the population. The simple approach to understand this problem lies in the following question

At the beginning of the spreading,
how many people do I infect before recovering?

If the answer is "*more than one*", then we have a cascade in which the propagation grows exponentially fast. If, on the opposite it is "*less than one*" than it dies out because, in most cases, every individual recovers before infecting someone else. We call this the *reproductive number*. As shown in Figure 2.2 it is the control parameter of a phase transition between a disease-free and an epidemic state.

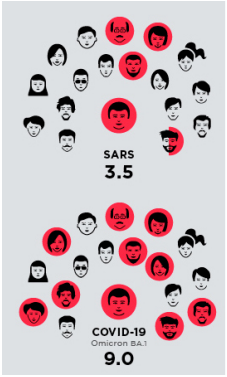

The effect of R_0, some numbers
Source:visualcapitalist.com/history-of-pandemics-deadliest/

Let us stress two important facts. The first one is that R_0 is defined *at the beginning* of the epidemic. Notation-wise, this is why we call it R_0, while R_t is the reproductive number at a given time t. This is important to say because the exponential spreading can occur only on a short time scale and then saturate due to the finite population size. The second fact is that the question refers to a non-better specified "I", implying that the answer is the same for everybody. Of course, if we think of our everyday life, the probability of infection vary a lot across individuals, according to their sociability, the interaction with children, the spaces they occupy *etc.* So, of course, we want an *average* answer and we will study it in the next section.

2.2 EPIDEMIC MODELING ON NETWORKS

As we mentioned, the epidemic spreading propagates through contacts that are well modeled by the edges of a graph. We now want to formally define the epidemic threshold transition for an arbitrary graph. This is of key importance to understand if, given the structure of the network and the disease parameters, the spread will touch a large fraction of individuals or not.

2.2.1 THE STATE EVOLUTION EQUATION

We consider an agent-based model in which every individual $i \in \mathcal{V}$ is associated to a discrete variable $x_i(t) \in \{S, I, R\}$ determining the state i is in. When a susceptible person i is in contact with an infectious one j ($A_{ij} = 1$) for a time dt, then it gets infected with a probability βdt. An infected person recovers with a probability μdt. We can write the probability of being infected at the time-step $t + dt$ as a function of t as follows:

The infected state equation of the SIR on a graph

$$\mathbb{P}(x_i(t+dt) = I) = \mathbb{E}\Bigg[\underbrace{\delta[x_i(t) = I](1-\mu)}_{i \text{ was infected and did not recover}} + \underbrace{\delta[x_i(t) = S]\left(1 - \prod_{j\in\mathcal{V}} \left(1 - \beta dt \cdot \delta[x_j(t) = I]\right)^{A_{ij}}\right)}_{i \text{ was susceptible and got infected}} \Bigg]. \tag{2.1}$$

This equation features two terms: the case in which i was susceptible and got infected and the can in which it was infected and did not recover. Note that the probability of being infected is written as 1 minus the probability of not being infected. We can simplify this equation in the limit for $dt \to 0$, focusing on the term describing the probability of not being infected.

$$\begin{aligned}
&\lim_{dt\to 0} \prod_{j\in\mathcal{V}} \left(1 - \beta dt \cdot \delta[x_j(t) = I]\right)^{A_{ij}} \\
&\overset{(a)}{=} \lim_{dt\to 0} \exp\left\{ \sum_{j\in\mathcal{V}} A_{ij} \log\left(1 - \beta dt \cdot \delta[x_j(t) = I]\right) \right\} \\
&\overset{(b)}{=} \lim_{dt\to 0} \exp\left\{ -\beta dt \sum_{j\in\mathcal{V}} A_{ij} \delta[x_j(t) = I] \right\} \\
&\overset{(c)}{=} \lim_{dt\to 0} 1 - \beta dt \sum_{j\in\mathcal{V}} A_{ij} \delta[x_j(t) = I],
\end{aligned}$$

where in (a) we used the identity $x = e^{\log x}$; in (b) we performed the expansion $\log(1+x) = x + o(x)$ and in (c) the expansion $e^x = 1 + x + o(x)$. Substituting this expression in Equation (2.1) we obtain

$$\begin{aligned}\mathbb{P}(x_i(t+dt) = I) &= \mathbb{E}\left[\delta(x_i(t) = I)\right](1-\mu) + \beta dt \sum_{j\in\mathcal{V}} A_{ij}\mathbb{E}\left[\delta[x_i(t) = S]\delta[x_j(t) = I]\right] \\ &= \mathbb{P}\left(x_i(t) = I\right)(1-\mu) + \beta dt \sum_{j\in\mathcal{V}} A_{ij}\mathbb{P}\left(x_i(t) = S, x_j(t) = I\right).\end{aligned}$$

Taking the first term on the right hand-side to the left and dividing by dt, we obtain the derivative of the probability that reads

$$\partial_t \mathbb{P}(x_i(t) = I) = \beta \sum_{j\in\mathcal{V}} A_{ij}\mathbb{P}\left(x_i(t) = S, x_j(t) = I\right) - \mu\mathbb{P}(x_i(t) = I). \tag{2.2}$$

Following the same passages, we get the evolution equations for all three states. Note that, $\partial_t\mathbb{P}(x_i(t) = S) + \partial_t\mathbb{P}(x_i(t) = I) + \partial_t\mathbb{P}(x_i(t) = R) = 0$, because the probability of being in one of the three states sums up to one.

SIR model on a graph

$$\begin{aligned}\partial_t \mathbb{P}(x_i(t) = S) &= -\beta \sum_{j\in\mathcal{V}} A_{ij}\mathbb{P}\left(x_i(t) = S, x_j(t) = I\right) \\ \partial_t \mathbb{P}(x_i(t) = I) &= \beta \sum_{j\in\mathcal{V}} A_{ij}\mathbb{P}\left(x_i(t) = S, x_j(t) = I\right) - \mu\mathbb{P}(x_i(t) = I) \\ \partial_t \mathbb{P}(x_i(t) = R) &= \mu\mathbb{P}(x_i(t) = I).\end{aligned} \tag{2.3}$$

In order to obtain the reproductive number we must study the stability of this system of equations that, however, is still non-linear and hard to study because it involves the marginal distributions $\mathbb{P}\left(x_i(t) = S, x_j(t) = I\right)$ for which we do not have an explicit expression. To cope with this problem, we adopt the simple naïve mean field approximation.

2.2.2 NAÏVE MEAN FIELD

The *naïve mean field* (NMF) approximation consists in considering all variables as independent *i.e.* in factorizing the marginals as follows

$$\mathbb{P}(x_i(t) = S, x_j(t) = I) = \mathbb{P}(x_i(t) = S)\mathbb{P}(x_j(t) = I). \tag{The NMF approximation}$$

This approximation greatly simplifies the problem. In fact, in (2.3) we have defined the evolution of $3n$ equations concerning the node marginal probabilities, but there are $2|\mathcal{E}|$ equations (where $\mathcal{E}$ is the set of edges) that are unspecified. Factorizing the probabilities with naïve mean field, we simply get rid of these terms. Let us first make some comments about this approximation, its limits and when we expect to be a good method to proceed.

Some notes on the naïve mean field approximation

Given its simplicity NMF is a commonly adopted strategy to first tackle a problem, but is it accurate? In other words, we are asking to what extent we can assume that the event that i is susceptible is independent from the event that its neighbor j is infected. Given the context of the model, the answer seems necessarily to be negative since the contagion is transmitted through the contacts.

The most relevant setting in which NMF should be considered is that of *dense* networks, *i.e.* those in which every node has a large degree. Suppose we have a fully connected network: the fact that the edge A_{ij} exists is simply irrelevant because all edges exist. One can show that indeed, in this setting the NMF approximation becomes asymptotically exact and, in general, the denser the network is the more the NMF approximation is accurate. An example of how to go beyond this approximation is discussed in chapter 3.

With NMF approximation at hand, Equation (2.2) turns into

$$\partial_t \mathbb{P}(x_i(t) = I) = \beta \mathbb{P}(x_i(t) = S) \sum_{j \in \mathcal{V}} A_{ij} \mathbb{P}(x_j(t) = I) - \mu \mathbb{P}(x_i(t) = I).$$

We now linearize this equation around the stationary state $\mathbb{P}(x_i(t) = S) = 1$ to get the reproductive number.

2.2.3 THE REPRODUCTIVE NUMBER WITH NAÏVE MEAN FIELD

As we explained before, we want to see the effect of perturbing the stationary state in which everybody is susceptible by adding a small probability of being infected. For simplicity, we denote $\mathbb{P}(x_i(t) = I) := p_i(t)$ and move to a vector form of the equations. We let $P_i(x_i(t) = S) = 1$ and obtain

The linearization around the diseases-free point under the NMF approximation

$$\partial_t \boldsymbol{p}(t) = (\beta A - \mu I_n) \boldsymbol{p}(t).$$

If we want that $\partial_t p_i(t) < 0$ for all i and all t, we must impose that $\beta \rho(A) - \mu < 0$, where $\rho(A)$ denotes the spectral radius of A. If this condition is satisfied, then we end up in the disease-free region. If on the opposite $\beta \rho(A) - \mu > 0$, the probability of being infected grows at each time step and the virus has a broad diffusion on the network. We thus obtain the following value for the reproductive number

Reproductive number with the NMF approximation

$$R_0 = \frac{\beta \rho(A)}{\mu} \tag{2.4}$$

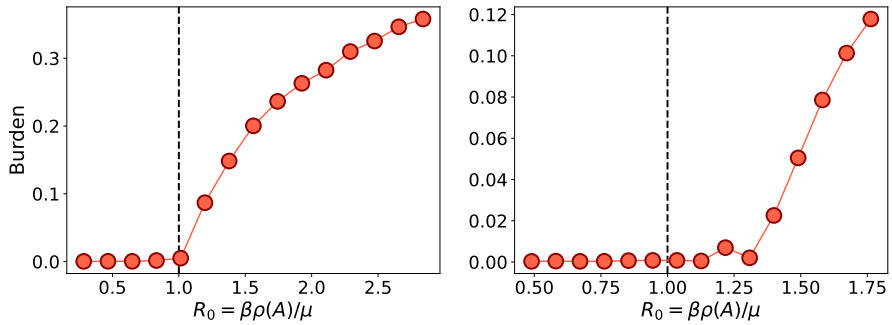

Figure 2.3: **Epidemic threshold: theoretical prediction versus simulated data**. We run a SIR model for different β values on a dense graph (left panel) and on a sparse one (right panel) generated from the random configuration model. We plot the burden (*i.e.* the fraction of non-susceptible individuals) as a function of R_0 as predicted by the NMF approximation.

In Figure 2.3 we compare this prediction with an empirical simulation on a dense (left panel) and on a sparse one (right panel), evidencing the goodness of the approximation only in the former case. Now, as a last step, we give some simple results relating the spectral radius of A with its structure.

2.2.4 GRAPH STRUCTURE AND REPRODUCTIVE NUMBER

Studying the spectral properties of the adjacency matrix for different generative models is a problem of great interest, that however goes beyond the scope of this course. Here we provide two simple examples with intuitive and non-rigorous arguments to characterize the value of $\rho(A)$ and understand the role of density and degree heterogeneity in determining the threshold.

Erdős Renyi random graph

The spectral behavior of the *Erdős-Rényi* (ER) random graph changes dramatically according to whether its expected average degree grows with its size or not. Letting p be the probability of being connected, then we can define two different regimes: the dense one in which $\log(n)/pn = o_n(1)$ and the sparse one in which the opposite is true, *i.e.* $pn/\log(n) = o_n(1)$. In words, if the average degree grows faster than $\log(n)$ we say the network to be *dense*. This is a game-changer because, under this hypothesis, the degree distribution is concentrated, *i.e.* , for all large n, with probability one

$$\max |d_i - np| = o_n(np).$$

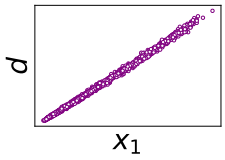

The leading eigenvalue of A, $\boldsymbol{x}_1$ against the degree vector on a random dense graph

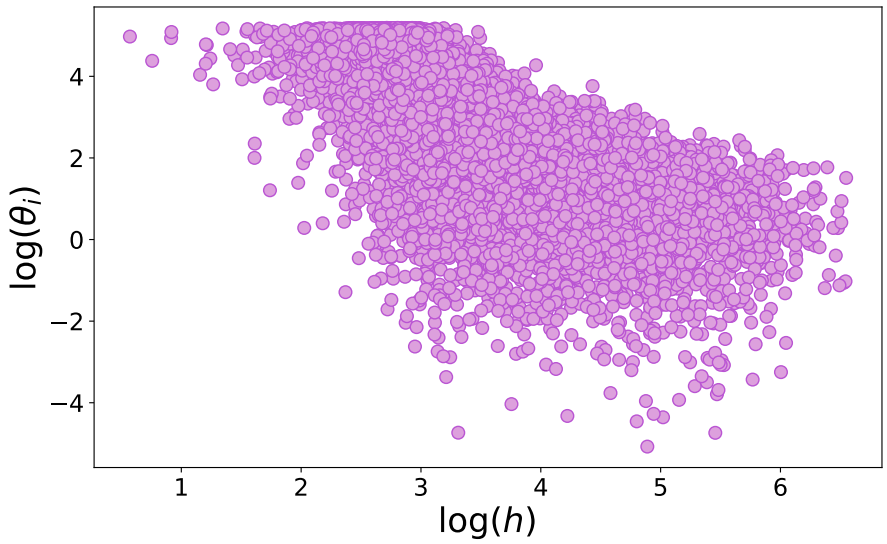

Figure 2.4: **Hitting time as a function of the expected degree**. We consider a random graph generated from the configuration model and denote with θ_i the expected degree of node i. In the plot we show the scatter plot of θ_i against the hitting time h, defined as the number of iterations after which the node got infected in a SIR simulation.

Again, in words, this means that a dense ER graph is quasi regular. In this case, we can heuristically[1] write the following equation

$\rho(A) = \langle d \rangle + o_n(d)$ *on dense ER graphs*

$$(A\mathbf{1}_n)_i = \sum_{j \in \mathcal{V}} A_{ij} = d_i \approx np \approx \langle d \rangle (\mathbf{1}_n)_i.$$

This implies that $\mathbf{1}_n$ is a close approximation of the leading eigenvector[2] and the average degree is an approximation of $\rho(A)$. From this result, we obtain that in denser networks an epidemic spreading runs faster, as one could reasonably expect.

Let us now consider the case in which the graph is generated from a configuration model with an arbitrary degree distribution.

Configuration model

Once again we operate under the assumption of being in a sufficiently dense regime and derive a heuristic expression of the leading eigenvector of A, which we suppose in this case to be $\boldsymbol{d}$, the degree vector.

$\rho(A) = \dfrac{\langle d^2 \rangle}{\langle d \rangle} + o_n(d)$

for dense random graphs with an arbitrary degree distribution

$$(A\boldsymbol{d})_i = \sum_{j \in \mathcal{V}} A_{ij} d_j \approx \sum_{j \in \mathcal{V}} \frac{d_i d_j^2}{2|\mathcal{E}|} = d_i \frac{\langle d^2 \rangle}{\langle d \rangle}.$$

We thus get that $\rho(A) = \langle d^2 \rangle / \langle d \rangle$ implying that a broad degree distribution makes the spreading run even faster on the network. This is because of the

1 For simplicity we derive this result heuristically, but it can be formally proved.
2 Due to Perron-Frobenius theorem.

role played by hubs, *i.e.* nodes with a high degree. Since they have a lot of connections, they are very likely to get infected in the earlier stages of the epidemic and then become super-spreaders. Notably, the value of $\rho(A)$ that we just may diverge for scale-free networks in which the second moment of the degree distribution goes to infinity, making the transition go to zero. Figure 2.4 shows for each node the infection hitting time (*i.e.* the time it takes to get infected) as a function of their degree. The plot evidences a strong negative correlation, confirming the intuition that nodes with a large degree are the first to get infected and then they are responsible of the spreading. Note that in practice the second moment of the degree may only diverge in the asymptotic theoretical limit. All real world networks are finite and so is $\langle d^2 \rangle$. Nonetheless, in real-world settings, it can be overwhelmingly large and drive the epidemic to unfold very fast on the network.

2.2.5 FROM THEORY TO PRACTICE: EPIDEMIC MITIGATION

Let us now discuss some basic facts about epidemic mitigation based on our results. Suppose we have a vaccine and we add a fourth compartment to our model, that of vaccinated people that behaves exactly like the recovered one. From our analytical view-point, we can still deploy the results we obtained, because vaccinated people simply do not take part to the process, since they cannot change their compartment. For this reason it is as if they were not part of the network.

We ask ourselves how vaccination impacts the epidemic spread. To answer this question we add a Boolean variable s_i the equals 0 if i is vaccinated and cannot transmit the disease and is 1 otherwise. The matrix that determines the epidemic threshold is then now

$$W = A \circ (\boldsymbol{s}\boldsymbol{s}^T).$$

Using a non-rigorous argument, we will see how the vaccination determines the epidemic threshold.

Methodological remark

The approach we used to study $\rho(A)$ was non rigorous but leads to the correct result because we assume A to be dense. By vaccinating a large portion of the population, instead W becomes sparse by design and not only the method we adopt but also the result is incorrect. Formally, we can only see what is the effect of vaccination on the spreading, assuming that a small fraction of the population has been vaccinated and W is still dense. This heuristic result, however, gives us some important intuition that we can verify numerically and that can be rigorously proved with other more rigorous methods.

Let $\tilde{d}_i = d_i s_i$. Then

$$\left(W\tilde{\boldsymbol{d}}\right)_i = \sum_{j\in\mathcal{V}} A_{ij} s_i s_j \tilde{d}_j \approx= \sum_{j\in\mathcal{V}} \frac{\tilde{d}_i d_j^2 s_j}{2|\mathcal{E}|} = \tilde{d}_i \frac{\boldsymbol{s}^T \boldsymbol{d}^2}{\mathbf{1}_n^T \boldsymbol{d}},$$

so $\frac{\boldsymbol{s}^T \boldsymbol{d}^2}{\mathbf{1}_n^T \boldsymbol{d}}$ is a close approximation of $\rho(W)$. Now, if s_i is Bernoulli random variable with probability p, we get

$$\rho(W) \approx p \frac{\langle d^2 \rangle}{\langle d \rangle}.$$

So, the vaccination decreases the R_0 and allows one to stay below the epidemic threshold. From a simple observation, however, one sees that this is not the optimal strategy. In fact, in we fix $\boldsymbol{s}^T \mathbf{1}_n$, *i.e.* the number of vaccines, and attempt to minimize $\boldsymbol{s}^T \boldsymbol{d}^2$ one immediately sees that the solution lies in vaccinating the nodes with the highest degree, *i.e.* the *hubs*. This target immunization significantly helps in improving the mitigation effectiveness.

2.3 EXTENSIONS

In the previous sections we only considered the SIR to model an epidemic spreading. While this is one the most relevant models in epidemiology, it must be mentioned that several alternatives exist. The simplest one is the SI in which individuals cannot recover and is equivalent to the SIR for $\mu = 0$. In this case one can see that no epidemic threshold exists and, for how little is the transmission parameter, the epidemic will certainly involve all the population sooner or later. Different is the case of the SIS model in which an infected individual recovers but is once again susceptible. This model accounts for the fact that having experienced an infection does not imply one is immune, in some cases. From a mathematical perspective this slightly changes things: as we commented already, in the SIR, an infected individual cannot have been infected by a susceptible neighbor. On the opposite in the SIS this can happen: a infected individual can have been infected by someone who *now* is susceptible but that recovered. Actually, the difference between these two regimes cannot be understood from the NMF approximation because it is indeed not able to capture this dynamic. If one adopts a more refined approximation strategy, however, it is indeed possible to see that in the two cases the epidemic threshold varies.

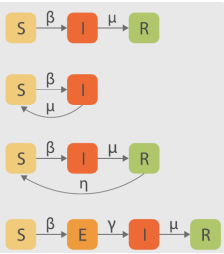

Other models realistically add more compartments to the equations. Some of the most common are the *exposed*, *vaccinated* and *dead* compartments. Exposed people are those who already contracted the virus but that are still not contagious. After some time, they turn infected. The addition of these or other compartments may take into account of more complex medical and behavioral factors. On top of this, the model parameters may add further

depth. We assumed β, μ to be constant and equal for all individuals, while one may assume that they depend, for instance, on age or mask-wearing.

It is worth mentioning that we only talked about simple contagion, *i.e.* the process in which one infected individual passes the disease over to a susceptible one. Thinking however of epidemiology in a broader sense, this is not the only possible alternative. Contagion may occur, for instance, only if one is exposed several times to an infected individual, each one passing a "piece". Only when all "pieces" are passed one becomes infected. Alternatively one can imagine contagion as a process in which it is necessary to have several infectious people interacting *at once* for the disease to be transmitted. We talk in these cases of *complex contagion*.

2.4 REFERENCES

- A.L. Barabasi, *Network Science, Chapter 10*, networksciencebook.com/chapter/10
  This chapter gives a wide and detailed view of epidemics on networks and can be used as a reading to get a bigger picture of the problem that we only treated in a very schematic way. From the analytical viewpoint, the book gives more results on the dynamics and considers also other models but does not use the NMF as it was presented here, but rather presents the degree-based mean field approach that is closely related to NMF.

- Pastor-Satorras, Castellano, Van Mieghem, Vespignani, *Epidemic processes in complex networks*, Reviews of modern physics 87.3 (2015): 925, arxiv.org/pdf/1408.2701.pdf
  This is a long but very important review. The intent of this review is less pedagogical that the Barabasi's book, but it takes a broader look at the problem from a technical perspective and summarizes different results.

- P. Van Mieghem, *Exact Markovian SIR and SIS epidemics on networks and an upper bound for the epidemic threshold*, arxiv.org/pdf/1402.1731.pdf
  This article details some rigorous results based on the NMF approximation with a notation very similar to the one adopted in this chapter.

3

CAVITY METHOD

3.1 SPARSE AND TREE-LIKE GRAPHS

In the previous lecture we introduced the *naïve mean field* (NMF) approximation to study the epidemic threshold on a graph. We saw, however, that this approximation is appropriate only for dense graphs, while most of real world graphs are (luckily) sparse. We here investigate an alternative approach that is well suited for sparse random graphs and that builds an approximation based on the locally tree-like[1] structure of a sparse *Erdős-Rényi* (ER) graph.

3.1.1 LOCALLY TREE-LIKE GRAPHS

Let us first introduce the concept of *rooted* graph $\mathcal{G}_i(\mathcal{V}, \mathcal{E})$ that is a graph in which a particular node $i \in \mathcal{V}$ (the *root*) is specified. Denote with $\mathfrak{B}_i(t)$ the ball of radius t around the node i, *i.e.* the sub-graph made by the set of all nodes that can be reached from i in at most t steps and the corresponding edges. If the law of $\mathfrak{B}_i(t)$ under uniformly random sampling of the root admits a limit $\mathcal{L}$, then we call it *local weak limit*. In words, $\mathcal{L}$ is the asymptotic local distribution of $\mathcal{G}(\mathcal{V}, \mathcal{E})$ as seen from a random vertex. A relevant result concerning sparse ER graphs[2] is that they locally converge to a tree, as more formally stated in Property 3.1.

1 We recall that an undirected graph $\mathcal{G}(\mathcal{V}, \mathcal{E})$is said to be a tree if it is connected and it does not contain any cycle.

2 But actually also other sparse random graphs.

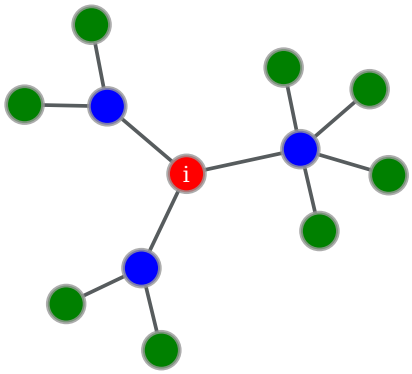

Figure 3.1: A toy example of a Poisson GW tree. In red the root i, in blue the first generation of nodes, in green the second.

Local convergence to a tree

Property 3.1 (Convergence to Poisson *Galton Watson tree* (GW) tree of ER)**.** *A* sparse *ER random graph with $n \to \infty$ rooted at i with average degree $d = O_n(1)$ converges locally to a Poisson GW tree so obtained: consider the node i as the root and generate d_i neighbours (called* sons*), where d_i is a Poisson random variable with parameter d and iteratively repeat the operation for each son.*

As a consequence of this property, a sparse ER graph locally *looks like* a tree and hence, with high probability, there are no cycles of finite size.[3] Figure 3.1 displays an example of a Poisson GW tree, rooted at i.

Let us now describe a fundamental property of probability distributions defined over the nodes of a tree, namely, *conditional independence.*

3.1.2 CONDITIONAL INDEPENDENCE

Consider three random variables x, y, z. We say that x and y are conditionally independent given z if

Conditional independence

$$\mathbb{P}[x, y \mid z] = \mathbb{P}[x \mid z]\mathbb{P}[y \mid z]. \tag{3.1}$$

Note that two random variables are independent if we can write $\mathbb{P}[xy] = \mathbb{P}[x]\mathbb{P}[y]$, that is what we did in the NMF approximation. Conditional independence holds only on the conditional probabilities and in general $\mathbb{E}[xy] \neq \mathbb{E}[x]\mathbb{E}[y]$. Now, the relation between conditional independence and trees is that all variables associated to the neighbors of a same node are conditionally independent given the value of their common neighbor, or, more formally

$$\forall j \neq k \in \partial i, \quad \mathbb{P}[x_j, x_k \mid x_i] = \mathbb{P}[x_j \mid x_i]\mathbb{P}[x_k \mid x_i].$$

Let us try to understand why. Suppose there is a piece of news that is propagating on the network through contacts. If a node knows it, then with some

3 Recall the local convergence definition is given in the asymptotic limit of $n \to \infty$. Finite cycles will exist, but their size will depend on n (for instance they may grow as $\log(n)$) and thus diverge in the large n limit.

probability it will talk about it to its neighbors that will also be aware of it from that moment on. Now, let us consider a node i (as the red one in Figure 3.1) and two of its neighbors j, k (in blue, same figure). If we let $x_i = 1$ if i knows the piece of information and $x_i = 0$ otherwise, then, clearly $\mathbb{P}[x_j, x_k] \neq \mathbb{P}[x_j]\mathbb{P}[x_k]$. If the variables were independent, the notion of x_j would not allow me to say anything about x_k, but it turns out that if I know x_j I can tell something about x_k. The two random variables bring information one of the other because there is a (short) path connecting them and the piece of information may flow from one node to the other. However, since we are considering a tree, there is only one such path, that is the one going through i. If we suppose to know x_i, then knowing also x_j does not add any information when trying to predict x_k, because the only influence j has on k is through i. This is the effect of conditional independence.

Notably, conditional independence implies the following relation that we will exploit later on.

$$\begin{aligned}\mathbb{P}(x_i, x_j, x_k) &= \mathbb{P}(x_j, x_k|x_i)\mathbb{P}(x_i) \\ &= \mathbb{P}(x_j|x_i)\mathbb{P}(x_k|x_i)\mathbb{P}(x_i) \\ &= \frac{\mathbb{P}(x_i, x_j)\mathbb{P}(x_i, x_k)}{P(x_i)}\end{aligned} \tag{3.2}$$

Knowing that a sparse ER random graph asymptotically "looks like" a tree, we can now simplify our analysis exploiting conditional independence and the graph structure to introduce the *cavity method*, or *belief propagation*.

3.2 FACTORIZING PROBABILITY DISTRIBUTIONS ON TREES

As we saw in Chapter 2, a difficulty of studying processes on a graph is to compute the edge marginal probability distributions that cannot be simply assumed to factorize as the product of the node marginals. The cavity method builds on the fact that the edge marginals can be exactly calculated on tree with a recursive formula, as stated in Lemma 3.1.

Lemma 3.1. *Let $\mathcal{G}(\mathcal{V}, \mathcal{E})$ be a tree and let $\mu(\boldsymbol{x})$ be a probability distribution defined on $\mathcal{G}(\mathcal{V}, \mathcal{E})$ that can be written as*

$$\mu(\boldsymbol{x}) = \prod_{(ij)\in\mathcal{E}} \phi_{ij}(x_i, x_j). \tag{3.3}$$

Then the edge marginal $\mu_{ij}(x_i, x_j) = \sum_{\boldsymbol{x}\setminus x_i, x_j} \mu(\boldsymbol{x})$ and the node marginal $\mu_i(x_i) = \sum_{\boldsymbol{x}\setminus x_i} \mu(\boldsymbol{x})$ can be written in the following form:

$$\mu_i(x_i) = \prod_{k\in\partial i} \eta_{ik}(x_i) \tag{3.4}$$

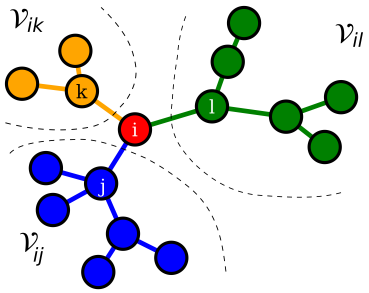

Figure 3.2: Sketch of a tree. The node i in red, while in green, blue and orange the edges and nodes $\mathcal{E}_{ix}, \mathcal{V}_{ix}$ with $x = j, k, l$, respectively. Note that i belongs to $\mathcal{V}_{ik}, \mathcal{V}_{ij}$ and $\mathcal{V}_{i\ell}$.

$$\mu_{ij}(x_i x_j) = \phi_{ij}(x_i, x_j) \prod_{k \in \partial i \setminus j} \eta_{ik}(x_i) \prod_{\ell \in \partial j \setminus i} \eta_{jl}(x_j). \tag{3.5}$$

The quantities $\eta_{ij}(x_i)$ are defined on the set of directed edges.

From Equations (3.4, 3.5), exploiting $\mu_i(x_i) = \sum_{x_j} \mu_{ij}(x_i, x_j)$, it is obtained that the *messages* have to satisfy the following fixed point equation

Message passing

$$\eta_{ij}(x_i) = \sum_{x_j} \phi_{ij}(x_i, x_j) \prod_{\ell \in \partial j \setminus i} \eta_{jl}(x_j). \tag{3.6}$$

Let us now sketch here the proof of Lemma 3.1 since it is very pedagogical and helpful to understand the essence of cavity method.

Proof of Lemma 3.1. Denote with $\mathcal{E}_d$ the set of directed edges of $\mathcal{G}(\mathcal{V}, \mathcal{E})$and consider $(ij) \in \mathcal{E}_{\mathrm{d}}$. We define $\mathcal{E}_{ij}$ as the set of all edges that can be reached from i only passing through j. As a consequence of the fact that on a tree there exists a unique path connecting any two nodes – since there are no cycles –, the two following properties are verified:

$$\forall\, i \in \mathcal{V}, \quad \mathcal{E} = \bigcup_{k \in \partial i} \mathcal{E}_{ik}\,; \tag{3.7}$$

$$\forall\, (ij) \in \mathcal{E}, \quad \mathcal{E} = \{(ij)\} \cup \underbrace{\bigcup_{k \in \partial i \setminus j} \mathcal{E}_{ik}}_{\text{reached from } (ji)} \cup \underbrace{\bigcup_{\ell \in \partial j \setminus i} \mathcal{E}_{jl}}_{\text{reached from } (ij)}. \tag{3.8}$$

Furthermore, note that $\forall\, j \neq k$, $\mathcal{E}_{ij} \cap \mathcal{E}_{ik} = \emptyset$. A pictorial representation of the definition of $\mathcal{E}_{ij}$ is given in Figure 3.2. Exploiting Equation (3.7), $\mu(\boldsymbol{x})$ can then be written as:

$$\mu(\boldsymbol{x}) = \prod_{(ab) \in \mathcal{E}} \phi_{ab}(x_a, x_b) = \prod_{k \in \partial i} \prod_{(ab) \in \mathcal{E}_{ik}} \phi_{ab}(x_a, x_b) := \prod_{k \in \partial i} \psi_{ik}(\boldsymbol{x}_{\mathcal{V}_{ik}}),$$

where $\mathcal{V}_{ik}$ is the set of nodes connected by edges in $\mathcal{E}_{ik}$ (i included) and $\boldsymbol{x}_{\mathcal{V}_{ik}}$ is the variable vector corresponding to those nodes. The node marginal can then be written in the following form

$$\mu_i(x_i) = \sum_{\boldsymbol{x}\setminus x_i} \mu(\boldsymbol{x}) = \sum_{\boldsymbol{x}\setminus x_i} \prod_{k\in\partial i} \psi_{ik}(\boldsymbol{x}_{\mathcal{V}_{ik}}) = \prod_{k\in\partial i} \sum_{\boldsymbol{x}_{\mathcal{V}_{ik}}\setminus x_i} \psi_{ik}(\boldsymbol{x}_{\mathcal{V}_{ik}}).$$

Denoting $\eta_{ik}(x_i) := \sum_{\boldsymbol{x}_{\mathcal{V}_{ik}}\setminus x_i} \psi_{ik}(\boldsymbol{x}_{\mathcal{V}_{ik}})$, we obtain the first equation of Lemma 3.1. Note that $\eta_{ki}(x_i)$ indeed only depends on x_i since the sum is run over all variables $\boldsymbol{x}_{\mathcal{V}_{ik}}$, except x_i. Proceeding in a similar way, the expression of the edge marginal is obtained from Equation (3.8).

$$\begin{aligned}
\mu_{ij}(x_i,x_j) &= \sum_{\boldsymbol{x}\setminus x_i x_j} \mu(\boldsymbol{x}) \\
&= \sum_{\boldsymbol{x}\setminus x_i x_j} \phi_{ij}(x_i,x_j) \prod_{k\in\partial i\setminus j} \prod_{(ab)\in\mathcal{E}_{ik}} \phi_{ab}(x_a,x_b) \prod_{\ell\in\partial j\setminus i} \prod_{(cd)\in\mathcal{E}_{k\ell}} \phi_{cd}(x_c,x_d) \\
&= \sum_{\boldsymbol{x}\setminus x_i x_j} \phi_{ij}(x_i,x_j) \prod_{k\in\partial i\setminus j} \psi_{ik}(\boldsymbol{x}_{\mathcal{V}_{ik}}) \prod_{\ell\in\partial j\setminus i} \psi_{j\ell}(\boldsymbol{x}_{\mathcal{V}_{j\ell}}) \\
&= \phi_{ij}(x_i,x_j) \left(\prod_{k\in\partial i\setminus j} \sum_{\boldsymbol{x}_{\mathcal{V}_{ik}}\setminus i} \psi_{ik}(\boldsymbol{x}_{\mathcal{V}_{ik}}) \right) \cdot \left(\prod_{\ell\in\partial j\setminus i} \sum_{\boldsymbol{x}_{\mathcal{V}_{j\ell}}\setminus j} \psi_{j\ell}(\boldsymbol{x}_{\mathcal{V}_{j\ell}}) \right) \\
&= \phi_{ij}(x_i,x_j) \prod_{k\in\partial i\setminus j} \eta_{ik}(x_i) \cdot \prod_{\ell\in\partial j\setminus i} \eta_{j\ell}(x_j).
\end{aligned}$$

□

The essence of the proof of Lemma 3.1 relies on the conditional independence of the node variables on trees. More specifically, to obtain Equation (3.7), one could imagine to remove the node i, obtaining d_i (the degree of i) disconnected sub-graphs in which variables are independent and hence factorize. Similarly Equation (3.8) is obtained removing the nodes i and j from the graph. We now show that on a tree, Equation (3.2) is verified.

Lemma 3.2. *Let $\mathcal{G}(\mathcal{V},\mathcal{E})$ be a tree and let $\mu(\boldsymbol{x})$ be a probability distribution defined on $\mathcal{G}(\mathcal{V},\mathcal{E})$ that can be written as per Equation (3.3). Then, taking $j,k\in\partial i$ with $j\neq k$ we can write*

$$\mathbb{P}(x_i,x_j,x_k) = \frac{\mathbb{P}(x_i,x_j)\mathbb{P}(x_i,x_k)}{\mathbb{P}(x_i)}$$

Proof. For simplicity, we will drop the dependence on the variables $\boldsymbol{x}$. Following the same procedure we used to prove Lemma 3.1, we can easily show that

$$\mathbb{P}(x_i,x_j,x_k) = \phi_{ij}\phi_{ik} \prod_{p\in\partial j\setminus i} \eta_{jp} \prod_{q\in\partial k\setminus i} \eta_{kq} \prod_{r\in\partial i\setminus\{j,k\}} \eta_{ir}.$$

This can be rewritten in the following form

$$\mathbb{P}(x_i, x_j, x_k) = \frac{\left(\phi_{ij} \prod_{p\in\partial j\setminus i} \eta_{jp} \prod_{r\in\partial i\setminus j} \eta_{ir}\right)\left(\phi_{ik} \prod_{q\in\partial k\setminus i} \eta_{kq} \prod_{r\in\partial i\setminus k} \eta_{ir}\right)}{\eta_{ik} \prod_{k\in\partial i\setminus k} \eta_{ir}}$$
$$= \frac{\mathbb{P}_{ij}(x_i, x_j)\mathbb{P}_{ik}(x_i, x_k)}{\mathbb{P}_i(x_i)},$$

where in the last step we used the relations shown in Lemma 3.1. □

Given these results on trees, let us now move to sparse graphs.

3.2.1 CAVITY METHOD ON TREE-LIKE GRAPHS

When we consider a graph that is not a tree, the proof we gave above does not generalize because $\mathcal{E}_{ij} \cup \mathcal{E}_{ik} \neq \emptyset$, due to the presence of cycles. In a tree-like graph, however, we know that cycles do not have a short length. When considering two nodes j, k in the neighborhood of a same node, there will be a short path of length 2 connecting them and other very long paths that pass through other nodes. The main intuition we have is that all those long paths are unimportant and the main channel of of relation is the short path connecting them. For this reason, we simply use conditional independence as an *ansatz* that is asymptotically verified on sparse graphs. We can then rewrite the cavity equations on a graph (with cycles) a follows.

Factorizing probabilities on sparse graphs

The cavity fixed point equations

$$\eta_{ji}(x_i) = \frac{Z_i}{Z_{ji}} \sum_{x_j} \phi_{ij}(x_i, x_j) \prod_{\ell\in\partial j\setminus i} \eta_{j\ell}(x_j).$$
$$\mu_i(x_i) \approx \frac{1}{Z_i} \prod_{k\in\partial i} \eta_{ik}(x_i)$$
$$\mu_{ij}(x_i, x_j) \approx \frac{1}{Z_{ij}} \phi_{ij}(x_i, x_j) \prod_{k\in\partial i\setminus j} \eta_{ik}(x_i) \prod_{\ell\in\partial j\setminus i} \eta_{j\ell}(x_j).$$

Given these equations, we now introduce the *non-backtracking matrix* or *Hashimoto operator* that naturally comes into play from the cavity method.

3.3 THE NON-BACKTRACKING MATRIX

Let us consider the fixed point cavity equation, letting $r_{ij}(x_i) = \log(\eta_{ij}(x_i))$ and $C_{ji} = \log(Z_i) - \log(Z_{ji})$.

$$r_{ji}(x_i) = C_{ji} + \log\left(\sum_{x_j} \exp\left\{\log \phi_{ij}(x_i, x_j) + \sum_{\ell \in \partial j \setminus i} r_{j\ell}(x_j).\right\}\right).$$

Focusing on the sum $\sum_{\ell \in \partial j \setminus i}$, we introduce the non-backtracking matrix.

The non-backtracking matrix

Let $\mathcal{E}_{\mathrm{d}}$ be the set of *directed* edges of a graph $\mathcal{G}$. We define the non-backtracking matrix $B \in [0,1]^{|\mathcal{E}_{\mathrm{d}}| \times |\mathcal{E}_{\mathrm{d}}|}$ as

$$B_{(ij),(k\ell)} = \delta_{jk}(1 - \delta_{i\ell}), \tag{3.9}$$

for all $(ij), (k\ell) \in \mathcal{E}_{\mathrm{d}}$. Then, given a vector $\boldsymbol{g} \in \mathbb{R}^{|\mathcal{E}_{\mathrm{d}}|}$, we have

$$(B\boldsymbol{g})_{(ij)} = \sum_{\ell \in \partial j \setminus i} g_{j\ell}.$$

The non-backtracking matrix is naturally related to the cavity method

In simple words, we can say that the non-backtracking matrix B is the linear operator associated to the cavity approximation. To interpret its definition, in essence we can see B as the adjacency matrix of graph in which each node is a directed edge of $\mathcal{G}(\mathcal{V}, \mathcal{E})$ and two nodes are neighboring if they are successive and the second one is not the reversed of the first. Unlike the adjacency matrix, the spectral radius of the non-backtracking matrix is "well behaved" in the sparse regime, as stated by the following theorem.

Theorem 3.1. *Consider a symmetric matrix $A \in [0,1]^{n \times n}$ in which the entries are set to 1 independently (up to symmetry) with probability $\mathbb{P}(A_{ij} = 1) = P_{ij}$ and $P_{ij} = O_n(n^{-1})$ for all i, j. Then, for all large n with high probability, the spectral radius of the non-backtracking matrix B associated with the adjacency matrix A is*

$$\rho(B) = \rho(P) + o_n(1).$$

This theorem is very general and allows us to consider easily both the ER and the configuration model. For the ER, we have $P = \frac{\langle d \rangle}{n} \mathbf{1}_n \mathbf{1}_n^T$ and $\rho(P) = \langle d \rangle$, the expected average degree. For the configuration model, instead, we can write $P = \frac{1}{2|\mathcal{E}|} \boldsymbol{d}\boldsymbol{d}^T$ and thus $\rho(B) = \frac{\langle d^2 \rangle}{\langle d \rangle}$.

Let us now see how the matrix B enters into play when studying the epidemic threshold on a sparse graph with the cavity method.

3.4 AN APPLICATION TO EPIDEMICS

Let us now use the cavity method to find the epidemic threshold on a sparse graph, in which the NMF is not appropriate. Let us consider Equation (2.2) that describes the dynamics of the infected state in a *Susceptible-Infected-Recovered model* (SIR) model. We can write

$$\partial_t \mathbb{P}(x_i(t) = I) = \beta \sum_{j \in \mathcal{V}} A_{ij} \mathbb{P}\left(x_i(t) = S, x_j(t) = I\right) - \mu \mathbb{P}(x_i(t) = I).$$

The whole point of going beyond NMF is to realize that $x_i(t), x_j(t)$ are not independent if $A_{ij} = 1$. To move forward, let us lighten a bit the notation. We define $\boldsymbol{p} \in \mathbb{R}^n$ the vector with entries $p_i(t) = \mathbb{P}(x_i(t) = I)$ and with $\boldsymbol{\chi}(t) \in \mathbb{R}^{2|\mathcal{E}|}$ the vector with entries $\chi_{ij}(t) = \mathbb{P}(x_i(t) = S, x_j(t) = I)$. Note that the vector $\boldsymbol{\chi}$ is defined over the set of *directed* edges of the graph and that $\chi_{ij}(t) \neq \chi_{ji}(t)$, in general. With this notation, we can rewrite the state evolution as

$$\partial_t \boldsymbol{p}(t) = \beta T \boldsymbol{\chi}(t) - \mu \boldsymbol{p}(t), \tag{3.10}$$

where we introduced the matrix $T \in \mathbb{R}^{n \times 2|\mathcal{E}|}$, defined as $T_{i,(ab)} = \delta_{ia} A_{ab}$. Now, to proceed, we need to write a state evolution equation for the vector $\boldsymbol{\chi}(t)$ as well. The probability that i and j are respectively susceptible and infected at a given time step implies that they were both susceptible and j got infected (but certainly not from i), while i did not or that j was already infected, it did not recover and i did not get infected.

$$\chi_{ij}(t + dt) =$$
$$\mathbb{E}\left[\delta[x_i(t) = S]\delta[x_j(t) = S] \underbrace{\left(1 - \beta dt \sum_{k \in \partial i \setminus j} \delta[x_k(t) = I]\right)}_{i \text{ does not get infected}} \underbrace{\beta dt \left(\sum_{\ell \in \partial j \setminus i} \delta[x_\ell(t) = I]\right)}_{j \text{ gets infected}}\right]$$
$$+ \mathbb{E}\left[\delta[x_i(t) = S]\delta[x_j(t) = I] \underbrace{\left(1 - \beta dt \sum_{k \in \partial i \setminus j} \delta[x_k(t) = I] - \beta dt\right)}_{i \text{ does not get infected}} \underbrace{(1 - \mu dt)}_{j \text{ recovers}}\right].$$

Now, there are two approximations we can perform to simplify the analysis. The first one is just to take the limit for $dt \to 0$ and remove the higher order terms. The second one is done exploiting conditional independence. We first remove the higher order terms in dt

$$\chi_{ij}(t + dt) \overset{dt \to 0}{=} \beta dt \left(\sum_{\ell \in \partial j \setminus i} \mathbb{E}\left[\delta[x_i(t) = S]\delta[x_j(t) = S]\delta[x_\ell(t) = I]\right]\right)$$

$$+\chi_{ij}(t)(1-\beta dt-\mu dt)-\beta dt\sum_{k\in\partial i\setminus j}\mathbb{E}\left[\delta[x_i(t)=S]\delta[x_j(t)=I]\delta[x_k(t)=I]\right].$$

We now exploit conditional independence. We denote with $\Omega_{ij}=\mathbb{P}(x_i(t)=S,x_j(t)=S)$ and $s_i=\mathbb{P}(x_i(t)=S)$ and write

$$\mathbb{E}\left[\delta[x_i(t)=S]\delta[x_j(t)=S]\delta[x_\ell(t)=I]\right]=\frac{\Omega_{ij}(t)\cdot\chi_{j\ell}(t)}{s_j(t)}$$
$$\mathbb{E}\left[\delta[x_i(t)=S]\delta[x_j(t)=I]\delta[x_k(t)=I]\right]=\frac{\chi_{ik}(t)\cdot\chi_{ij}(t)}{s_i(t)},$$

thus turning the state evolution equation into

$$\chi_{ij}(t+dt)\overset{dt\to0}{=}\beta dt\frac{\Omega_{ij}(t)}{s_j(t)}\sum_{\ell\in\partial j\setminus i}\chi_{j\ell}(t)+\chi_{ij}(t)(1-\beta dt-\mu dt)-\beta dt\frac{\chi_{ij}(t)}{s_i(t)}\sum_{k\in\partial i\setminus j}\chi_{ik}(t).$$

To get the epidemic threshold we now want to linearize around the epidemic-free fixed point that is $\Omega_{ij},s_i,s_j\to1$ and $\chi_{ij}\to0$ and get

$$\chi_{ij}(t+dt)\overset{dt\to0}{=}\beta dt\sum_{\ell\in\partial j\setminus i}\chi_{j\ell}(t)+\chi_{ij}(t)(1-\beta dt-\mu dt),$$

that can be written as

$$\partial_t\boldsymbol{\chi}(t)=(\beta B-(\beta+\mu)I_{2|\mathcal{E}|})\boldsymbol{\chi}(t).$$

Injecting this result in Equation (3.10)

$$\begin{pmatrix}\partial_t\boldsymbol{p}(t)\\ \partial_t\boldsymbol{\chi}(t)\end{pmatrix}=\begin{pmatrix}-\mu I_n & \beta T\\ \beta B-(\beta+\mu)I_{2|\mathcal{E}|} & 0\end{pmatrix}\begin{pmatrix}\boldsymbol{p}(t)\\ \boldsymbol{\chi}(t)\end{pmatrix}.$$

From a simple calculation one sees that the stability condition is now obtained on heterogeneous random graphs as

The reproductive number according to the cavity method

$$R_0=\frac{\beta(\rho(B)-1)}{\mu}=\frac{\beta}{\mu}\left(\frac{\langle d^2\rangle}{\langle d\rangle}-1\right).$$

If we compare this result with the one obtained from NMF, the main difference is the appearance of the term "-1" that accounts the fact that when there is a susceptible-infected pair (ij), certainly i did not infect j. This comes "for free", in the sense that we did not have to add this correction manually and it naturally came from the equations. Other than that the results seem quite similar, but we must not forget that $\rho(A)$ is very close to $\rho(B)$ on dense networks but not on sparse ones. In other words, $\frac{\langle d^2\rangle}{\langle d\rangle}$ still is the good quantity to look at, but it is actually not the spectral radius of A in the sparse regime. Using the method explained in Chapter 2, we can derive the R_0 of the SIR model in the presences of vaccination. Note that, while with NMF this

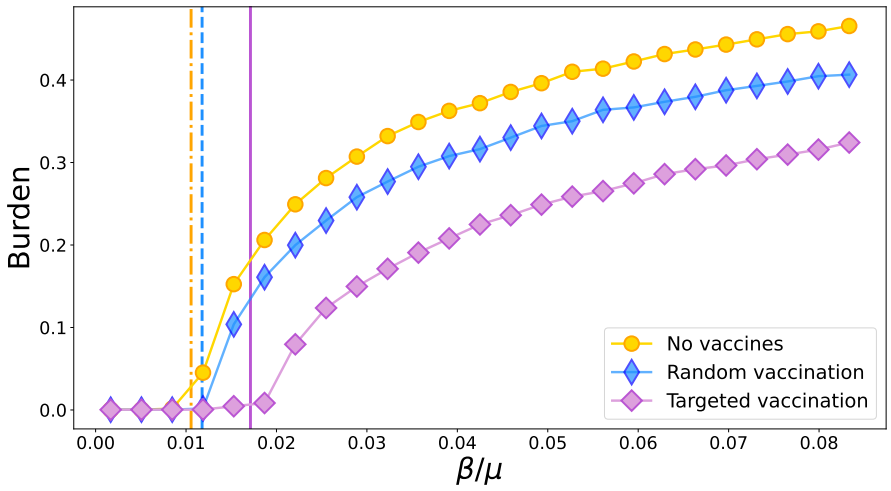

Figure 3.3: **Epidemic burden as a function of β/μ for different vaccination strategies**. The yellow dots are the burden (fraction of non-susceptible people at the end of the simulation) in absence of vaccination; the blue diamonds correspond to the random vaccination; the purple squares are the targeted vaccination in which each person is vaccinated with a probability proportional to the degree. The vertical lines (color coded) correspond to the position of the transition as predicted by the cavity method for the three different scenarios.

result was not rigorous because the effect of vaccination is to sparsify the network, with the cavity method we obtain e precise bound. The simulation shows the goodness of the cavity method in this setting as well as the efficacy of targeted vaccination strategies, as shown in Figure 3.3, we introduce $Q_{i,(ab)} = \delta_{ib}A_{ab}$ and $M_{(ab),(cd)} = A_{ab}A_{cd}\delta_{bc}\delta_{ad}$.

3.5 EFFICIENTLY COMPUTING THE SPECTRAL RADIUS OF B

We have seen that the non-backtracking matrix naturally appears when adopting the cavity approximation. The B matrix defined in Equation (3.9) however is large (its size scales with the number of edges, not of nodes) and it might not be so straightforward to build. However, we now show that there is a matrix B_{p} of size $2n \times 2n$ whose eigenvalues are also eigenvalues of B and it is much more easily built. Similarly to the matrix T introduced earlier $T_{i,(ab)} = \delta_{ia}A_{ab}$, we introduce $Q \in \mathbb{R}^{n\times 2|\mathcal{E}|}$ and $M \in \mathbb{R}^{2|\mathcal{E}|\times 2|\mathcal{E}|}$

$$\begin{aligned} Q_{i,(ab)} &= \delta_{ib}A_{ab} \\ M_{(ab),(cd)} &= \delta_{bc}\delta_{ad}A_{ab}A_{cd}. \end{aligned}$$

Now, the following relations[4] are satisfied:

4 You may try to obtain these relations as an exercise.

$$
\begin{aligned}
Q^T T - M &= B \\
TQ^T &= A \\
QQ^T &= D \\
QM &= T \\
TM &= Q
\end{aligned}
$$

With these relations at hand, suppose $\boldsymbol{g}$ is the leading eigenvector of B with eigenvalue ρ, then

$$\rho T\boldsymbol{g} = TB\boldsymbol{g} = T(Q^T T - M)\boldsymbol{g} = AT\boldsymbol{g} - Q\boldsymbol{g},$$

and

$$\rho Q\boldsymbol{g} = QB\boldsymbol{g} = Q(Q^T T - M)\boldsymbol{g} = DT\boldsymbol{g} - T\boldsymbol{g}.$$

Denoting $P\boldsymbol{g} = \boldsymbol{x}$ and $Q\boldsymbol{g} = \boldsymbol{y}$ for simplicity, we obtain,

$$\underbrace{\begin{pmatrix} A & -I_n \\ D - I_n & 0 \end{pmatrix}}_{B_{\mathrm{P}}} \begin{pmatrix} \boldsymbol{x} \\ \boldsymbol{y} \end{pmatrix} = \rho \begin{pmatrix} \boldsymbol{x} \\ \boldsymbol{y} \end{pmatrix}, \tag{3.11}$$

where we introduced the smaller matrix $B_{\mathrm{P}} \in \mathbb{R}^{2n \times 2n}$. This matrix has the same eigenvalues as B (except those equal to ± 1 that have a different degeneracy). This matrix can thus be used to efficiently compute $\rho(B)$.

3.6 CONCLUSION

In this section we introduced the cavity method and the closely related non-backtracking matrix. Unlike the NMF approximation, this method is well suited for sparse graphs, being asymptotically exact on sparse random graphs, such as the ER. Consequently, this "second order" approximation (in which we assume independence at the edge, rather than the node level) is more accurate, but we must recall that real-world networks are often sparse but not locally tree-like. Sparse random graphs, in fact, tend to have a much smaller clustering coefficient than a real network with the same average degree. The low clustering coefficient, however, implies the absence of short loops, making the cavity method exact on random, but not on real world graphs, in general. This approximation is a improvement over NMF approach that is appropriate to deal with some of its limitations.

3.7 REFERENCES

- Wainwright, Jordan: *Graphical Models, Exponential Families, and Variational Inference*

This review is a milestone for physics methods on graphs and in Chapter 4 it treats the cavity method.

- Mezard, Montanari: *Information, Physics and Computation.*
  This is another relevant reference. The cavity method is discussed in Chapter 14.